

Transaction-Oriented Dynamic Power Flow Tracing for Distribution Networks—Definition and Implementation in GIS Environment

Eduardo Vega-Fuentes¹, Member, IEEE, Jin Yang², Senior Member, IEEE, Chengwei Lou, and Nand K. Meena, Senior Member, IEEE

Abstract—There is a growing interest from owners of distributed energy resources (DERs) to actively participate in the energy market through peer-to-peer (P2P) energy trading. Many strategies have been proposed to base P2P energy trading on. However, in those schemes neither the costs of assets usage nor the losses incurred are so far taken into account. This article presents a transaction-oriented dynamic power flow tracing (PFT) platform for distribution networks (DNs) implemented in a geographic information system (GIS) environment. It introduces a new transaction model that quantifies the use of the DN, apportions the losses and unlocks a flexible use of the surplus generation enabling that prosumers can adopt simultaneously different mechanisms for participation in energy trading, maximizing renewable energy usage. The platform is also helpful for future distribution system operators (DSOs) to overcome the status invisibility of low voltage (LV) DNs, determine who makes use of the assets, debit the losses on them and explore the effects from new connections. A case study is conducted over the IEEE European LV Test Feeder. The tool provides a clear, intuitive, temporal and spatial assessment of the network operation and the resulting power transactions, including losses share and efficiency of DERs.

Index Terms—Distribution networks, dynamic power flow tracing, geographic information system, P2P energy simulation platform.

NOMENCLATURE

B_n	Bus (node) n .
\mathcal{B}	Set of all buses in \mathcal{H} .
\mathcal{E}	Set of all lines (edges) in \mathcal{H} .
\mathcal{G}	Set of all buses with generation.
G_x	Power injection (generator, substation, battery discharging) number x .

GG	Number of power injections in \mathcal{H} .
\mathcal{H}	Radial low voltage distribution network.
I_i^p	Current injected in bus i , phase p .
\mathcal{L}	Set of all buses with a load.
L_{i-j}	Line from bus i to bus j .
LL	Number of lines in \mathcal{H} .
Lo_y	Power sink (load, battery charging) number y .
$Loss_{G_x-Lo_y}$	Losses incurred due to transaction $G_x - Lo_y$.
$Loss_{i-j}$	Losses in line L_{i-j} .
P_{G_x}	Active power generated by G_x .
$P_{G_x-Lo_y}$	Active power transferred in transaction $G_x - Lo_y$.
$P_{Rem-G_x}^t$	Active power not traded (remaining) by G_x at time t .
P_{i-j}	Active power inflow from line L_{i-j} .
PO_{i-j}	Active power outflow through line L_{i-j} .
S_i^p	Complex power.
$T_{G_x}^t$	Set of all transactions agreed by G_x at time t .
V_i^p	Complex voltage at bus i , phase p .
γ_{ij}^{pq}	Element of the admittance matrix.
ξ_{G_x}	Generator G_x performance index.
$\xi_{G_x-Lo_y}$	Transaction $G_x - Lo_y$ performance index.
Γ	Set of all the lines involved in transactions.
$\pi_{G_x-Lo_y}^t$	Ask price from prosumer G_x in its transaction with load Lo_y at time t .
π_{FIT}	Feed-in tariff price.
$\gamma_g^{p,Lo}$	Power share from generator g to load Lo , phase p .
$\gamma_g^{p,L_{i-j}}$	Power share from generator g in line L_{i-j} , phase p .
$\gamma_{Lo_y}^{p,L_{i-j}}$	Power share to load Lo_y in line L_{i-j} , phase p .

Manuscript received January 22, 2020; revised May 27, 2020 and September 15, 2020; accepted October 20, 2020. Date of publication October 26, 2020; date of current version February 26, 2021. This work was supported by the Engineering and Physical Sciences Research Council (EPSRC), U.K. Research and Innovation (UKRI), U.K. under Grant EP/S001778/2 “Street2Grid—An Electricity Blockchain Platform for P2P Energy Trading.” Paper no. TSG-00105-2020. (Corresponding author: Eduardo Vega-Fuentes.)

Eduardo Vega-Fuentes, Jin Yang, and Chengwei Lou are with the James Watt School of Engineering, University of Glasgow, Glasgow G12 8QQ, U.K. (e-mail: eduardo.vega-fuentes@glasgow.ac.uk; jin.yang@glasgow.ac.uk; 25440351@student.gla.ac.uk).

Nand K. Meena is with the School of Engineering and Applied Science, Aston University, Birmingham B4 7ET, U.K. (e-mail: n.meena@aston.ac.uk).

Color versions of one or more of the figures in this article are available online at <https://ieeexplore.ieee.org>.

Digital Object Identifier 10.1109/TSG.2020.3033625

I. INTRODUCTION

POLICIES toward decarbonization aiming at a climate-neutral society by 2050, technology development and improvements in the components required (power electronics, batteries and advanced metering infrastructure) and the growing acceptance of new control strategies including demand side programs, augur a substantial increase in the adoption of distributed energy resources (DERs), including distributed generation, energy storage and electric vehicles considering vehicle to grid (V2G) technology [1].

Energy demand in the network might be more efficiently managed with DERs participating actively in the energy market [2]. This could benefit the power system by maximizing renewable energy penetration, shaving peak load and reducing losses, electricity network operational costs and asset upgrade investments [3].

The traditional mechanism for participation of prosumers (proactive consumers with flexible loads, local power generation or storage facilities) in energy trading is through feed-in tariffs (FiT) [4], which enable the sale of the generation excess to the grid. This means, for the U.K. case, that a small photovoltaic (PV) system, i.e., 4 kW, would get an export price of 5.50 p/kWh (pence per kWh) [5]. Meanwhile, the import price with a standard domestic demand tariff would be 17.493 p/kWh [6]. The FiT scheme export tariff in U.K. closed to new entrants from 31 March 2019 while the smart export guarantee (SEG) came into force in January 2020 [7]. SEG is an obligation set by the Government for licensed electricity suppliers to offer a tariff and make payment to small-scale low-carbon generators for any electricity exported to the grid. The precise details of tariff (length, level, whether a flat rate or varying according to the time of day electricity is generated, etc.) are for suppliers to decide. However, payment greater than zero at all times of export is guaranteed, including when prevailing wholesale prices are negative. Most of the currently offered SEG tariffs are fixed, standing in a range between 1.0 and 5.6 p/kWh. To date, there is only one supplier in U.K. offering variable tariffs pegged to half-hourly wholesale rate.

A. Power Flow Tracing and P2P Energy Trading

Given the disparity between energy import rates and export FiT/SEG tariffs, prosumers would increase their economic profit trading their generation surplus with neighboring consumers [8]. This idea led to the peer-to-peer (P2P) energy trading concept, an innovative energy management technique that enable prosumers to actively participate in the energy market by selling or buying energy directly with each other without intermediators [9].

Many strategies have been proposed to base P2P energy trading on. In [10] a double-auction market with multiple buyers and sellers is designed to allow selling an amount of stored energy to customers in need of energy. Liu *et al.* [11] introduced an energy sharing provider to coordinate the trading. In [12] the trade is contract based to cope with asymmetric information and encourage prosumers participation. A coalitional game among cooperating prosumers is used in [13] to derive the price of electricity. However, these schemes do not take into account neither the costs of assets usage nor the losses.

From the distribution network operator (DNO) perspective, as P2P energy traders make use of the distribution network (DN) and affect its operation, transactions could be charged with a fee. This fee should be mostly based on usage. In this situation, the power flow tracing (PFT) techniques are useful to determine the path followed by the streams of power flowing from every DER to the loads through the DN. This

article presents PFT tools to identify the assets involved in a particular transaction and quantify their usage.

In the establishment of a fair P2P energy trading environment, it has to be accepted that not all the power injected by a generator reaches the loads. While the consumer will only be minded to pay for the power supplied, the seller will need to account for the losses in order to estimate the power required and determine the sale price. The PFT techniques presented in this work allow determining the share of losses incurred in the network by a given transaction between a DER and a load.

On the other hand, some agreed transactions might not be feasible. Unlike any other trade of goods, electricity trade is hardly dependent on technical constraints imposed by the network and an uncoordinated usage of the grid might compromise its operation. Therefore, physical network constraints must be included in energy trading models [14].

B. PFT Implementation and Geographic Information System

DNs were designed to send power outwards, not to accept significant net infeed from local generation. High DER penetration in low voltage (LV) DNs will affect voltage, phase balance, direction of energy flows, protection mechanisms and load profiles, requiring enhanced operations coordination at the transmission/distribution interfaces [15]. Most DERs are not visible to the system operator and do not follow a dispatch signal. This lack of visibility and control is becoming an important challenge for operations in DER-rich networks [16], making the management of LV networks increasingly difficult [17].

Although still in the initial stages with operational responsibilities and market models yet to be defined, functions of future distribution system operators (DSOs) should include processing interconnection requests, acting as the balancing entity for load and generation, coordinating the electricity sale and purchase, managing the power exchange among markets, and controlling resources output [18]. All these tasks could be efficiently managed with PFT tools.

As DER deployment spreads, assuming their variable performance in both time and locations (for the case of V2G), not only is needed studying their behavior over time, but also spatial analysis is required. In this article, a geographic information system (GIS) environment is proposed and implemented to add spatial visualization and perception to the dynamic power flows in complex DNs.

GIS provides a spatial context to manage data, perform analysis and create foresight [19]. By organizing data in layers on top of a map, new insights can be gained and solutions to complex business issues can be inferred. Furthermore, a GIS platform provides direct perception of information that is self-evident for non-experts. Typical GIS applications refer to asset management and workforce routing support for recovery from outages. Other applications have been reported on power systems including suitability assessments for renewable energies [20]–[22], planning of transmission lines, substations and DNs [23]–[25] and even detection and location of non-technical losses due to altered data of energy consumption in smart meters application database [26].

This trend and the need of integrating power flow calculations in a GIS environment have been recognized: in [27] the behavior of prosumers is automated using optimal power flow based on differential evolution and coupled with a GIS for dynamic visualization; Valverde *et al.* [28] developed two software plugins to integrate a distribution system simulator within a GIS platform allowing smart grid techniques in large-scale DNS being explored.

Dynamic PFT in a GIS environment is an innovative approach to facilitate DSOs to have a grasp of what is happening in the network, overcoming the status invisibility of LV DNS. It enables assessing the impact of a particular generator or load on the distribution system, determining which transactions are making use of assets, their quantified share, the losses they are responsible for and charging them on the basis of facilities used.

From the trading point of view, displaying power transactions would enable and encourage transparent P2P engagements among prosumers, maximizing renewable energy usage. The GIS platform with integrated power flow calculations, assesses the impact of DERs and prevents from congestion and constraint violations, enhancing the feasibility.

The platform presented combines two open-source software packages: OpenDSS (electric power distribution systems simulator) [29] and Quantum GIS (QGIS, GIS platform) [30]. The QGIS Python console (PyQGIS) [31] carries out the generation of all dynamic scenarios, and controls OpenDSS while driving time series simulations, calculates the PFT and generates information layers for GIS presentations.

In summary, the contributions of this article are as follows:

- A transaction-oriented dynamic PFT for DNS is proposed and implemented in a GIS environment. P2P energy trading is called to be disruptive to the conventional DN operation and management but to the best of our knowledge not any P2P energy trading mechanism existing in literature quantifies the usage of the distribution system or accounts for the losses.
- With the GIS environment for the first time, the visibility of power flow traces is explored from all DERs to loads; the numerous power transactions are displayed; the assets involved are tracked and the losses caused are accounted enabling transparent P2P energy trading.
- A new transaction model is defined and supported in PFT where losses are apportioned in the power transactions existing in the network. This model unlocks flexible use of the surplus generation. It enables prosumers to engage in P2P transactions with part of their production and sale the remaining power to the grid simultaneously.
- It is proposed that the generators and transactions are ranked based on their performance with newly defined efficiency indices which are helpful for prosumers to decide the mechanism for participation in energy trading.
- The feasibility is validated for energy transactions, in an angle from preventing violation to the network constraints or compromising normal DN operations.

The rest of this article is organized as follows. Section II introduces the proposed dynamic DN-PFT including the adopted loss allocation procedure, with a validation assessment

using the IEEE-33 Bus distribution circuit and the power flow tracing algorithm deployed. Section III describes the dynamic energy transactions model. Section IV details the platform architecture to implement the DN-PFT model. Section V shows a case study demonstration on the IEEE European LV Test Feeder. Finally, Section VI presents the concluding remarks.

II. DEFINING DYNAMIC DN-PFT

Power flow tracing is based on the proportional sharing (PS) principle [32], which assumes that nodes in the network are perfect ‘mixers’ of incoming flows proportionally shared among the nodal outflows. However, assessing the contributions of individual generators to individual loads depends on loss allocation. Losses through lines are nonlinear functions of current, therefore power flow through lines cannot be directly apportioned among generators.

Many loss allocation procedures have been proposed to deal with the costs of transmission and distribution networks operation. In [33], three families of proposed procedures for transmission networks (TNs) are reported: pro-rata (PR) procedures, marginal procedures and PS procedures. In PR procedures, losses are globally assigned to generators and consumers, then a proportional allocation rule is used: the losses allocated to a generator (consumer) are proportional to its corresponding level of energy generation (consumption). In marginal procedures, losses are assigned through the so-called incremental transmission loss coefficients followed by a normalization to restore over-recovery. In PS based procedures, power flows through lines are assumed to be an average over the sending- and receiving-end flows and by adding half of the line loss to the power injections at each terminal node of the line.

A. DN-PFT Preliminaries

Procedures developed for TNs require specific adaptations to be applied to DNS [34]. These systems differ in many respects, being them the R/X ratio of lines, load characteristics and behavior profiles, injection/consumption of reactive power by end users, etc.

A variety of new loss allocation methods for DNS rest on the marginal and PR loss allocation procedures, including quadratic [35], [36], direct loss coefficient [37] and circuit theory-based methods [38], [39]. Often, the aim of these methods is allocating losses fairly, e.g., benefiting DERs which contributed for loss reduction. However, regarding PFT for which only physics matters, the sole purpose of loss allocation is dealing with losses when applying PS to fit the shares of incoming flows among the nodal outflows.

Considering the simple representative system displayed in Fig. 1, where Po_{i-j} is the power outflow from bus B_i through the line L_{i-j} , Pi_{i-j} is the power inflow in bus B_j from line L_{i-j} , and $Loss_{i-j}$ are the losses in line L_{i-j} . If 100% of losses are allocated by the generators’ side, the contribution from G_1 to the load Lo_1 would be $[70/(70 + 30)] \times 100\% = 70\%$ and the remaining 30% would be fed from G_2 .

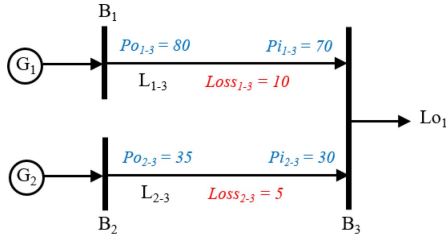


Fig. 1. Illustration of power contributions of generators based on loss allocation.

At the other extreme, if 100% of losses are allocated by the loads' side, the contribution from G_1 to the load would be $[80/(80 + 35)] \times 100\% = 69.56\%$ and 30.44% from G_2 . Whichever PR based loss allocation procedure is chosen, it would result in a contribution from G_1 in between the two extreme allocation approaches, i.e., 69.56% and 70%. Thus, the contribution from these generators applying PS method, results in $[75/(75+32.5)] \times 100\% = 69.77\%$ from G_1 and 30.23% from G_2 .

In practice, so far, losses in DNs are allocated by the utility side. Furthermore, in P2P energy trading, consumers would only accept paying for the power supplied. The seller would be responsible for the losses, accounting them as costs in determining the sale price. Thus, for our dynamic DN PFT we use the PR procedure with 100% of losses allocated to generators or power injections (e.g., at secondary substation transformers). A validation for this assumption is detailed in the next subsection.

B. PR Procedure Verification in the IEEE 33-Bus System

Unlike TNs, in LV DNs wire lengths are shorter and having less power flowing through them. Hence losses are not huge and there would be no significant difference in the PFT results obtained by deploying any of the allocation procedures. This remark is verified by comparing the contributions of generators to active power consumption of loads using different procedures over the IEEE 33-Bus distribution test circuit.

The IEEE 33-Bus circuit is one of the most discussed distribution test system available in literature, supporting many DN loss allocation research papers, including [34], [38]. Here it is used as a benchmark to compare PFT results allocating losses by the generator side, by loads side and using PS.

The layout is shown in Fig. 2. Lines and loads data are defined in [40]. To assess PFT, this 12.66 kV circuit is modified by adding 3 generators connected to Buses 14 (G_1 , 753.90 kW and 365.13 kVAr), 24 (G_2 , 1099.30 kW and 532.41 kVAr) and 30 (G_3 , 1071.30 kW and 518.85 kVAr) as in [38]. The total power demand is 3.715 MW and 2.3 MVar. The generators powering the lines are also depicted in the figure using different colors. Most lines are powered only by one source, but L_{3-4} to L_{5-6} fed by the secondary substation in blue and G_2 in red, and L_{6-7} to L_{7-8} powered by the secondary substation, G_2 and G_3 . It may be observed that loads connected to Bus 8 receive power from all four sources in the network.

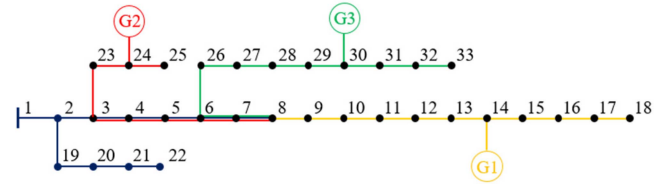


Fig. 2. Modified IEEE 33-Bus distribution test system for DN-PFT.

TABLE I
MODIFIED IEEE 33-BUS POWER SHARE MATRIX

	100% Generator			PS			100% Loads					
	S/S	G_1	G_2	G_3	S/S	G_1	G_2	G_3	S/S	G_1	G_2	G_3
L_{3-4}	0.674	0	0.326	0	0.675	0	0.325	0	0.675	0	0.325	0
L_{4-5}	0.674	0	0.326	0	0.675	0	0.325	0	0.675	0	0.325	0
L_{5-6}	0.674	0	0.326	0	0.675	0	0.325	0	0.675	0	0.325	0
L_{6-7}	0.422	0	0.204	0.374	0.421	0	0.203	0.376	0.421	0	0.202	0.377
L_{7-8}	0.422	0	0.204	0.374	0.421	0	0.203	0.376	0.421	0	0.202	0.377

The losses through lines with this configuration are found to be 19.6 kW. The comparison of loss allocation using these PR extreme methods is presented in Fig. 3, where PS results are always in between losses allocated to the sending node and to the receiving one.

Table I presents the resulting power share matrix (share of power from each generator in every line) with the three loss allocation methods in the lines powered by more than one source, where S/S refers to the secondary substation.

The results verify that the losses are not huge and that there is no significant difference to PFT when deploying any of the PR based loss allocation procedures. From the PFT point of view, allocating them by the sending node is rather intuitive as only the power reaching the receiving node is accounted. Thus, it is the adopted method for the following proposed dynamic DN-PFT.

C. DN-PFT Model

Consider a radial three-phase unbalanced LV DN $\mathcal{H}(\mathcal{B}, \mathcal{E})$ consisting of a set of buses \mathcal{B} and a set of distribution lines (edges) \mathcal{E} . It is operating in sinusoidal steady state. We index the buses by $i = \{1 \dots N\}$, where the root of the radial network (bus 1) represents the secondary substation and it is considered the slack bus. The generator buses are collected in the set $\mathcal{G} = \{1 \dots G\} \subseteq \mathcal{B}$ and the load buses in the set $\mathcal{L} = \{1 \dots Lo\} \subseteq \mathcal{B}$. A line in \mathcal{E} is denoted by the buses it connects L_{i-j} .

According to Kirchoff's Current Law, the relation between the injected currents I and the bus voltages V , is described by the admittance matrix Y :

$$I = Y \cdot V; \begin{bmatrix} I_1^{abc} \\ \vdots \\ I_N^{abc} \end{bmatrix} = \begin{bmatrix} Y_{11}^{abc} & \dots & Y_{1N}^{abc} \\ \vdots & \vdots & \vdots \\ Y_{N1}^{abc} & \dots & Y_{NN}^{abc} \end{bmatrix} \cdot \begin{bmatrix} V_1^{abc} \\ \vdots \\ V_N^{abc} \end{bmatrix} \quad (1)$$

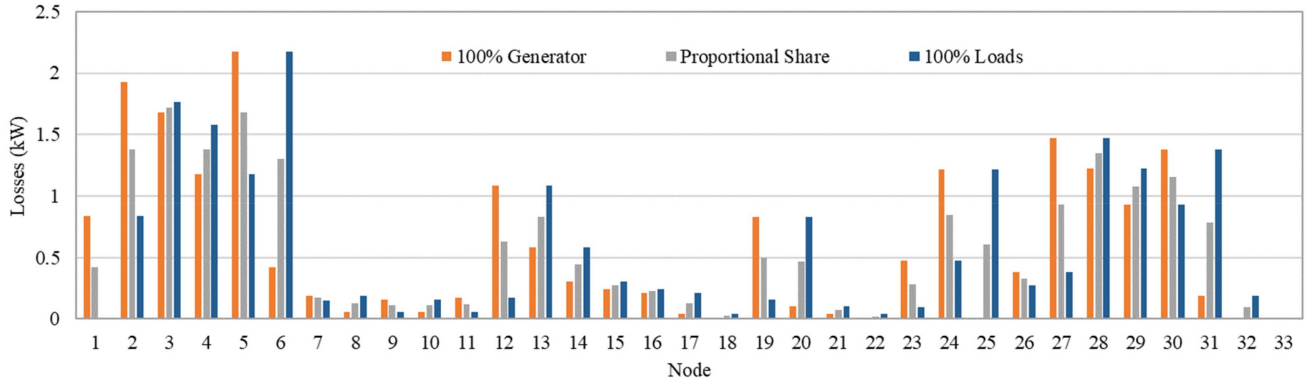


Fig. 3. Comparison of loss allocation to 100% generator, PS, and 100% loads.

In (1) I_i^{abc} , Y_{ij}^{abc} and V_i^{abc} are given as:

$$I_i^{abc} = \begin{bmatrix} I_i^a \\ I_i^b \\ I_i^c \end{bmatrix}; Y_{ij}^{abc} = \begin{bmatrix} Y_{ij}^{aa} & Y_{ij}^{ab} & Y_{ij}^{ac} \\ Y_{ij}^{ba} & Y_{ij}^{bb} & Y_{ij}^{bc} \\ Y_{ij}^{ca} & Y_{ij}^{cb} & Y_{ij}^{cc} \end{bmatrix};$$

$$V_i^{abc} = \begin{bmatrix} V_i^a \\ V_i^b \\ V_i^c \end{bmatrix} \quad (2)$$

where I_i^p is the injected current, V_i^p is the complex voltage at bus i for a given phase $p(a, b, c)$ and Y_{ij}^{pq} is the element of the admittance matrix. The injected current $I_i^{\hat{p}}$ at bus i for a given phase \hat{p} can be computed as:

$$I_i^{\hat{p}} = \sum_{k \in \mathcal{B}} \sum_{q \in \mathcal{P}} Y_{ik}^{\hat{p}q} \cdot V_k^q \quad (3)$$

The per phase assessment stands for the single-phase nature of most loads and DERs in LV DN.

The equations for the three-phase power flow are given by:

$$S_i^{\hat{p}} = V_i^{\hat{p}} \cdot (I_i^{\hat{p}})^* = V_i^{\hat{p}} \cdot \sum_{k \in \mathcal{B}} \sum_{q \in \mathcal{P}} (Y_{ik}^{\hat{p}q})^* \cdot (V_k^q)^* \quad (4)$$

where $S_i^{\hat{p}}$ is the injected complex power. It is decomposed into real (\Re) and imaginary (\Im) parts as follows:

$$S_i^{\hat{p}} = P_i^{\hat{p}} + jQ_i^{\hat{p}} \quad (5)$$

Tracing power address the problem of breaking down the power injection of a particular generator into constituent parts that serve loads and is incurred in losses through lines. Specifically, we decompose the active power injected $P_g^{\hat{p}}$ by the generator g , as the linear combination:

$$P_g^{\hat{p}} = \sum_{Lo \in \mathcal{L}} \gamma_g^{\hat{p}, Lo} \cdot P_{Lo}^{\hat{p}} + \sum_{l \in \mathcal{E}} \gamma_g^{\hat{p}, l} \cdot Loss_l^{\hat{p}} \quad (6)$$

The coefficients $\gamma_g^{\hat{p}, Lo}$ and $\gamma_g^{\hat{p}, l}$ refer to the shares of power of load Lo and losses in line l supplied by generator g in phase \hat{p} . They are computed by direct application of the PS principle to every mixing bus, i.e., the bus receiving inflows from different sources. $P_{lo}^{\hat{p}}$ is the active power consumption of load lo and $Loss_l^{\hat{p}}$ are the losses in line l , both in phase \hat{p} .

The share of power, $\gamma_g^{\hat{p}, L_{i-j}}$, of a generator g , in phase \hat{p} , in line L_{i-j} is given in (7) and expressed by the ratio of the active power incoming from generator g to all active power injected in the line, multiplied by the power share in line L_{h-i} also powered by g (the power share in lines fed by g only, would be 1). With the radial nature of the network, there will only be one path from the generator to the line. Knowing the lines powered by each generator is a key factor when using this equation. This calculation must start from the generator and continue downstream towards the loads.

The share of power from a generator in a load will be the same as the share of power from that generator in the last line supplying the load.

We also approximate the share of losses from a generator in a line to the share of power supplied by the generator through it. This statement is supported by the PR losses allocation assumption. Therefore, in our model a generator is liable for the same share of losses in a line as the share of power from that generator served through the line.

$$\begin{aligned} \gamma_g^{\hat{p}, L_{i-j}} &= \gamma_g^{\hat{p}, L_{h-i}} \frac{\Re(V_i^{\hat{p}} \cdot \sum_{q \in \mathcal{P}} (Y_{ig}^{\hat{p}q})^* \cdot (V_g^q)^*)}{P_i^{\hat{p}}} \\ &= \gamma_g^{\hat{p}, L_{h-i}} \frac{\Re(V_i^{\hat{p}} \cdot \sum_{q \in \mathcal{P}} (Y_{ig}^{\hat{p}q})^* \cdot (V_g^q)^*)}{\Re(V_i^{\hat{p}} \cdot \sum_{k \in \mathcal{B}} \sum_{q \in \mathcal{P}} (Y_{ik}^{\hat{p}q})^* \cdot (V_k^q)^*)} \\ &= \gamma_g^{\hat{p}, L_{h-i}} \frac{\Re(\sum_{q \in \mathcal{P}} (Y_{ig}^{\hat{p}q})^* \cdot (V_g^q)^*)}{\Re(\sum_{k \in \mathcal{B}} \sum_{q \in \mathcal{P}} (Y_{ik}^{\hat{p}q})^* \cdot (V_k^q)^*)} \\ &= \gamma_g^{\hat{p}, L_{h-i}} \frac{\Re(I_i^{\hat{p}, g})}{\Re(I_i^{\hat{p}})} \quad (7) \end{aligned}$$

The concepts introduced so far are illustrated over the circuit in Fig. 5 (Section III). Where the shares of power from G_1 using (7) yield:

$$\begin{aligned} \gamma_{G_1}^{L_{1-3}} &= 30/(30 + 70) = 0.30 \\ \gamma_{G_1}^{L_{2-3}} &= 0/(42) = 0 \\ \gamma_{G_1}^{L_{3-4}} &= 0.30 \times 80/(80 + 20) = 0.24 \end{aligned}$$

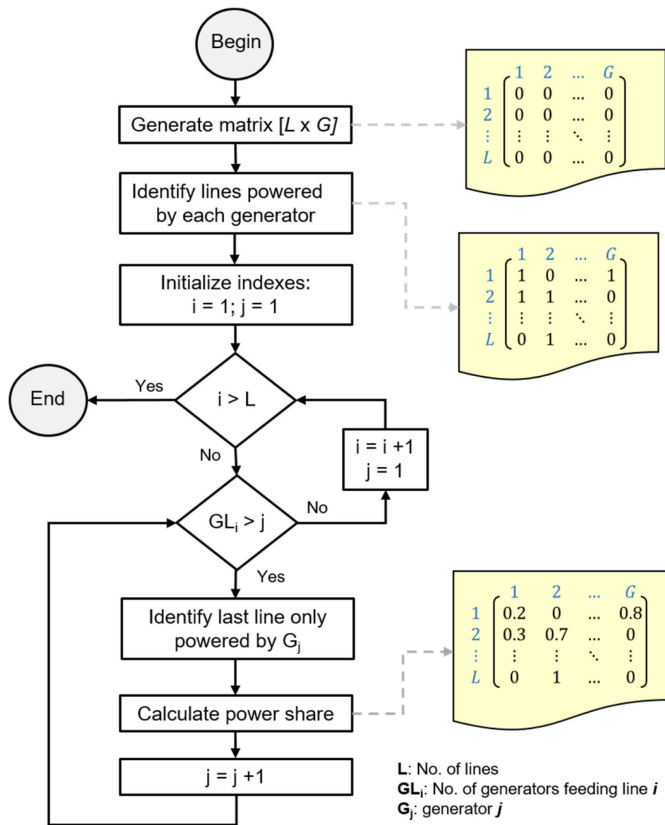


Fig. 4. Proposed dynamic power flow tracing algorithm.

and the active power injected by G_1 is decomposed using (6) in:

$$P_{G_1(\text{servng loads})} = 0.30 \times 15 + 0 \times 20 + 0.24 \times 30 + 0.24 \times 60 = 26.1$$

$$P_{G_1(\text{losses incurred})} = 0.30 \times 5 + 0 \times 2 + 0.24 \times 10 = 3.9.$$

D. Dynamic DN-PFT Implementation

Fig. 4 shows the algorithm proposed to dynamically trace the power flowing at every time step and split it among generators. Indices are used to loop the power share assessment in a line from every generator (j) and for all lines (i). The single-phase nature of generators and consumers in LV networks requires the process to be applied three times, one for each phase. Three-phase loads and generators are split and accounted in all three calculations.

Determining lines powered by a given generator is a process supported by power flow calculations at each time step. Starting from the connection point for each generator, lines with outflows are selected. Then the nodes at the end of those lines are analyzed and again, lines connected to them with outflows are selected. This process continues until no more outflows exist.

Table II summarizes the results obtained by applying this methodology to the demonstration energy transaction benchmark circuit (Fig. 5).

TABLE II
LINES POWERED BY EACH GENERATOR IN THE BENCHMARK CIRCUIT

	GENERATOR		
	G_1	G_2	G_3
L_{1-3}	1	1	0
L_{2-3}	0	0	1
L_{3-4}	1	1	1

TABLE III
POWER SHARE MATRIX OF THE BENCHMARK CIRCUIT

	GENERATOR		
	G_1	G_2	G_3
L_{1-3}	0.3	0.7	0
L_{2-3}	0	0	1
L_{3-4}	0.24	0.56	0.2

In reckoning the power share in lines powered by more than one generator, the last line (or bus) exclusively powered by each generator has to be identified. Then, assuming that electricity is indistinguishable and each of the outflows downstream the line from the bus depends only on the voltage gradient and impedance of the line, it may be assumed that each kW leaving the node contains the same proportion of the inflows as the total nodal flow. For instance, line L_{3-4} from the circuit in Fig. 2 is fed by generators G_1 , G_2 and G_3 . The outflowing power at B_3 (bus 3) is the sum of 20 kW from L_{2-3} (powered only by G_3) plus 80 kW from L_{1-3} (powered by G_1 and G_2). In L_{3-4} the power share from G_2 is $[20/(20+80)] \times 100\% = 20\%$, and as in line L_{1-3} the power share from G_1 is $[30/(30+70)] \times 100\% = 30\%$ and from G_2 is $[70/(30+70)] \times 100\% = 70\%$, the power share in L_{3-4} from G_1 is $[80/(20+80)] \times 30\% = 24\%$ and from G_2 the remaining 56%.

The algorithm results in a matrix sized $[LL \times GG]$, where LL is the number of lines and GG is the number of power injections in the network. It is filled in with the power share of each line from every generator. Table III presents the resulting power share matrix for the energy transaction benchmark circuit in Fig. 5.

The procedure to assess power shares in loads is the same as that for outflowing lines connected to the same bus. By means of the power share matrix the power in load Lo_3 (30 kW) can be traced, resulting in 24% provided by G_1 (7.2 kW), 56% by G_2 (16.8 kW) and 20% by G_3 (6 kW). The loads fed by a particular generator can be traced as well, e.g., G_1 feeds 30% of Lo_1 (15 kW, connected to B_1 and with the same share as L_{1-3}), 24% of Lo_3 (30 kW, connected to B_3 and with the same share as L_{3-4}) and 24% of Lo_4 (60 kW, connected to B_4 and with the same share as L_{3-4}); 26.1 kW in total. The remaining 3.9 kW generated by G_1 become losses in lines.

III. DYNAMIC DN-PFT ENERGY TRANSACTION MODEL

Consider the energy transaction benchmark circuit shown in Fig. 5, with three generators G_1 , G_2 and G_3 producing 30 kW,

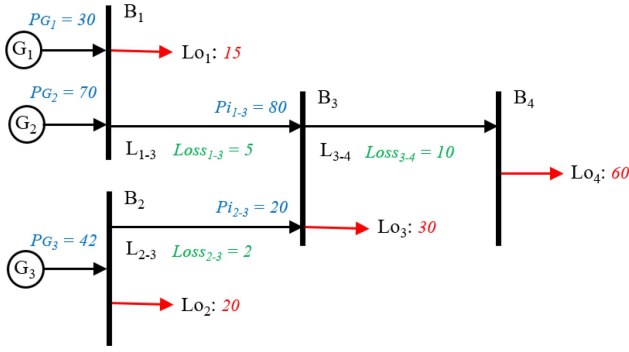


Fig. 5. Benchmark circuit for demonstrating the DN-PFT energy transaction model.

 TABLE IV
TRANSACTIONS BREAKDOWN

	TRANSACTIONS (kW)								
	G_1-L_{01}	G_1-L_{03}	G_1-L_{04}	G_2-L_{01}	G_2-L_{03}	G_2-L_{04}	G_3-L_{02}	G_3-L_{03}	G_3-L_{04}
$Loss_{1-3}$	0	0.45	1.05	0	1.05	2.45	0	0	0
$Loss_{2-3}$	0	0	0	0	0	0	0	0.6	1.40
$Loss_{3-4}$	0	0	2.40	0	0	5.60	0	0	2
Total Losses	0	0.45	3.45	0	1.05	8.05	0	0.6	3.40
Power transferred	4.5	7.2	14.4	10.5	16.8	33.6	20	6	12
	$G_1: 26.1$			$G_2: 60.9$			$G_3: 38$		

70 kW and 42 kW respectively. There are four loads and three lines. Losses in lines are displayed in green. The number of energy transactions amounts 9 and can be easily accounted by the number of generators feeding directly the bus where the load is connected ($G_1 - Lo_1$, $G_2 - Lo_1$ in B_1 and $G_3 - Lo_2$ in B_2) or powering the line feeding the bus ($G_1 - Lo_3$, $G_1 - Lo_4$, $G_2 - Lo_3$, $G_2 - Lo_4$, $G_3 - Lo_3$ and $G_3 - Lo_4$, with G_1 , G_2 and G_3 feeding B_3 with Lo_3 and powering line L_{3-4} feeding B_4 where Lo_4 is connected).

The lines involved in a particular transaction are tracked upstream from the bus where the load is connected, looking for lines powered by the generator in that transaction. The power share matrix will sort the losses assessment for each transaction as well as the power transferred. Table IV breaks down the transactions, including the lines involved, their loss shares and the power generated that reaches the loads.

The total losses incurred by a generator in phase \hat{p} can be obtained by means of (8), where the set $\Gamma = \{L_{i-j} \in G_x - Lo\}$ includes all the lines powered by G_x , $\gamma_{G_x}^{\hat{p}, L_{i-j}}$ is the power share from G_x in line L_{i-j} calculated with (7) and $Loss_{L_{i-j}}^{\hat{p}}$ are the losses in line L_{i-j} .

$$Loss_{G_x} = \sum_{l \in \Gamma} \gamma_{G_x}^{\hat{p}, l} \cdot Loss_l^{\hat{p}} \quad (8)$$

The losses due to a particular transaction are given by (9), where the set $\Gamma_y = \{L_{i-j} \in G_x - Lo_y\}$ includes all the lines powered by G_x involved in the transaction ($G_x - Lo_y$), $\gamma_{Lo_y}^{\hat{p}, L_{i-j}}$ is the power share to load Lo_y in line L_{i-j} calculated with (10). Its calculation requires knowing the power share in the next line in the path to the load L_{j-k} , therefore this calculation

must start from the load and upstream to the generator.

$$Loss_{G_x - Lo_y} = \sum_{l \in \Gamma} \gamma_{G_x}^{\hat{p}, l} \cdot Loss_l^{\hat{p}} \cdot \gamma_{Lo_y}^{\hat{p}, l} \quad (9)$$

$$\begin{aligned} \gamma_{Lo_y}^{\hat{p}, L_{i-j}} &= \gamma_{Lo_y}^{\hat{p}, L_{j-k}} \frac{\Re(V_i^{\hat{p}} \cdot \sum_{q \in P} (Y_{iLo_y}^{\hat{p}q})^* \cdot (V_{Lo_y}^q)^*)}{P_i^{\hat{p}}} \\ &= \gamma_{Lo_y}^{\hat{p}, L_{j-k}} \frac{\Re(V_i^{\hat{p}} \cdot \sum_{q \in P} (Y_{iLo_y}^{\hat{p}q})^* \cdot (V_{Lo_y}^q)^*)}{\Re(V_i^{\hat{p}} \cdot \sum_{k \in B} \sum_{q \in P} (Y_{ik}^{\hat{p}q})^* \cdot (V_k^q)^*)} \\ &= \gamma_{Lo_y}^{\hat{p}, L_{j-k}} \frac{\Re(\sum_{q \in P} (Y_{iLo_y}^{\hat{p}q})^* \cdot (V_{Lo_y}^q)^*)}{\Re(\sum_{k \in B} \sum_{q \in P} (Y_{ik}^{\hat{p}q})^* \cdot (V_k^q)^*)} \\ &= \gamma_{Lo_y}^{\hat{p}, L_{j-k}} \frac{\Re(I_i^{\hat{p}, Lo_y})}{\Re(I_i^{\hat{p}})} \quad (10) \end{aligned}$$

The sum of losses due to all transactions participated by a generator equal the losses incurred by that generator.

$$Loss_{G_x} = \sum_{G_x - Lo_y \in G_x - Lo} Loss_{G_x - Lo_y} \quad (11)$$

In light of the breakdown in Table IV, two efficiency indices are defined: the transaction performance index (12), defined as the ratio in percentage of the power transferred to the sum of the power transferred plus the total losses in the transaction; and the generator performance index (13), defined as the ratio in percentage of the power transferred in all transactions participated by the generator to its total power generated.

Transaction performance index:

$$\xi_{G_x - Lo_y} = \frac{P_{G_x - Lo_y}}{P_{G_x - Lo_y} + Loss_{G_x - Lo_y}} \cdot 100\% \quad (12)$$

Generator performance index:

$$\xi_{G_x} = \frac{\sum P_{G_x - Lo_y}}{P_{G_x}} \cdot 100\% = \frac{P_{G_x} - Loss_{G_x}}{P_{G_x}} \cdot 100\% \quad (13)$$

The performance indices for transactions and generators in the circuit from Fig. 5 are presented in Table V. They depend on the network topology and on the losses. Thus, generators connected to the same bus injecting different power have the same performance index and take part in transactions with the same efficiency. The most efficient transactions are those with the load closer to the generator, those with less losses through lines. The number of transactions and the performance indices vary during the day with load and generation profiles.

In the most market-effective P2P energy trading scenario, peers will prefer the most efficient available transactions. The proposed performance indices provide a ranking for efficient transactions, thereby helpful for peers to decide, for instance, whether DERs should store the power generated, engage in P2P trading or decline some proposals and combine trading mechanisms, i.e., part of the generation devoted to P2P trading and Fit/SEG for the remaining power.

TABLE V
PERFORMANCE INDICES

Index	TRANSACTION								
	$G_1-L_0_1$	$G_1-L_0_3$	$G_1-L_0_4$	$G_2-L_0_1$	$G_2-L_0_3$	$G_2-L_0_4$	$G_3-L_0_2$	$G_3-L_0_3$	$G_3-L_0_4$
$\zeta_{G_x-L_{0y}}$	100%	94.11%	80.67%	100%	94.11%	80.67%	100%	90.91%	77.92%
ζ_{G_x}	$G_1: 87\%$			$G_2: 87\%$			$G_3: 90.47\%$		

A. Trading Mechanisms Combination

Not all the generation excess produced by a DER has to be traded in P2P transactions, sold to the grid through FiT/SEG or stored. DN-PFT unlocks combination, a flexible use of the surplus generation.

With DN-PFT power transactions and due losses incurred are unequivocally identified. This means that if a prosumer only sells a part of its generation excess in P2P transactions, it still could access the FiT/SEG for the remaining power or store it for a future trade or on-site use.

The remaining power at a given time is given by:

$$P_{Rem-G_x}^t = P_{G_x}^t - \sum_{y \subset T_{G_x}^t} (P_{G_x-L_{0y}}^t + Loss_{G_x-L_{0y}}^t) \quad (14)$$

where $T_{G_x}^t$ includes all P2P energy transactions agreed by G_x at a given time t .

DN-PFT is also helpful for prosumers to determine the minimum ask price for sellers. It would be that producing the same income than FiT/SEG, and would be calculated as:

$$\pi_{G_x-L_{0y}}^t \geq \frac{P_{G_x-L_{0y}}^t + Loss_{G_x-L_{0y}}^t}{P_{G_x-L_{0y}}^t} \cdot \pi_{FiT} \quad (15)$$

where $\pi_{G_x-L_{0y}}^t$ is the ask price for prosumer G_x in its potential transaction with load L_{0y} at time t and π_{FiT} is the FiT/SEG price.

In Fig. 6 the red line represents the income resulting from trading the power excess with the grid through FiT/SEG. The prosumer's income for different ask prices are depicted in blue. The minimum ask price for a power injection P (power transaction + losses incurred) would be p_0 producing the same income than with the FiT/SEG. Trading with an ask price p_1 would increase the income for the prosumer, as shown in the figure.

Notice that as the injected power increases, the losses grow with the square of the current and the share of power reaching the load drops. Trading more power than P , asking π_0 will generate less income to the prosumer than participating with FiT/SEG. Therefore, there is a trade-off between the amount of power that is being traded and the usage of the network. Based on the proposed DN-PFT future research can be carried out about the optimization of the prosumers' trading strategies and outcomes considering feasible P2P transactions, their performance and FiT/SEG to determine ask prices and base for decision making.

IV. DN-PFT GIS IMPLEMENTATION PLATFORM

The DN-PFT GIS platform presented in this article is implemented with two open-source software packages: OpenDSS

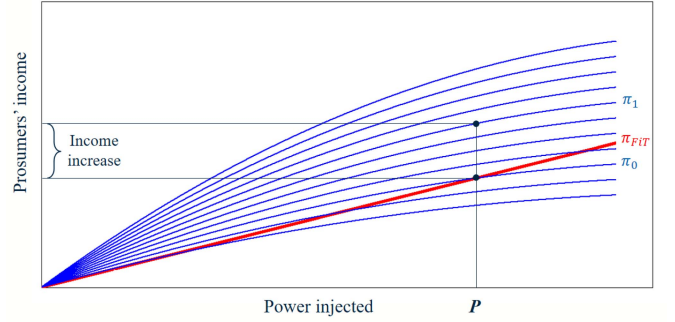


Fig. 6. Income increase comparison with FiT/SEG and P2P energy trading.

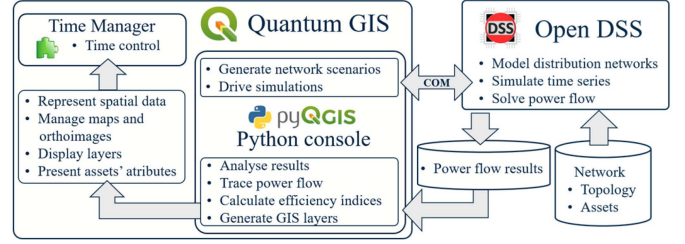


Fig. 7. DN-PFT platform architecture and simulation implementation.

and QGIS. The derived dynamic DN-PFT tool can be launched alone or combined with other software packages [41] to incorporate flexibility, customization ability and accessibility which are desirable attributes for modern power systems analysis tools.

Fig. 7 depicts the functions carried out by each of the software packages and the interfaces between them. All network scenarios are generated in the QGIS Python console (PyQGIS). It also controls the OpenDSS power flow calculations through the COM interface, analyzes the results, traces the power flows and generates the GIS layers for every time step. QGIS represents the spatial data, displaying the layers over maps and orthoimages. It also presents assets attributes.

Once all calculations are performed, results are split among phases to prevent from overlapping representations. Then, three different points of view (POV) are available: generators, loads and DSO. From generators' POV, it is a valuable ability to trace each power injection throughout the network, presenting the flow to loads with a narrowing width proportional to the power. From loads' POV the platform displays the generators and the flows powering the selected loads only. Finally, the DSO's POV aims assessing network utilization. Power flows from all generators are shown at the same time. Flows are merged producing lines colored by the combination of the power inflows colors.

Layers are created for every time step, then the Time Manager plugin for QGIS [42] adds the capability to animate vectors based on time attributes, enabling browsing through spatial-temporal data.

V. PLATFORM DEMONSTRATION – CASE STUDY

A case study was performed with the IEEE European LV Test Feeder [43] to demonstrate the implementation. This circuit consist of 55 single-phase loads with 1-minute resolution



Fig. 8. Power flow tracing from pv51 in the modified IEEE European LV Test Feeder at 12:30 pm.

TABLE VI
 DERs IN THE MODIFIED IEEE EUROPEAN LV TEST FEEDER

	Lo 5	Lo 14	Lo 22	Lo 30	Lo 31	Lo 48	Lo 51	Lo 52
Max Load (kW)	3.438	2.471	1.833	3.044	8.297	8.894	3.566	8.267
Daily consumption (kWh)	6.949	5.389	4.896	6.809	6.931	10.703	8.302	5.848
PV size (kWp)	2.4	1.8	1.5	2.4	2.4	3.3	2.7	1.8

profiles. 21 loads are connected to phase *a*, 19 to phase *b* and 15 to phase *c*. Fig. 8 plots the circuit layout over an orthoimage in the GIS platform. The blue triangle points the secondary substation and loads in phase *a* are represented with circles.

We included 8 PVs in the circuit (red circles in Fig. 8) with different sizes based on the daily average consumption, but with the same generation profile (assumed same solar irradiation).

Table VI presents the maximum power, the average consumption and the power of the PV panels installed by the prosumers.

In Table VII the transactions and the share of power from each source are tabulated from two snapshots at 12:30 pm and at 5 pm. It shows the contributions from DERs feeding each load. For instance, Load 25 at 12:30 pm is supplied completely by pv30, while at 5 pm it is fed 92.1% from pv30 and 7.9% by pv31. From generator’s POV, pv51 feeds at 12:30 pm loads 1 (21.5%), 3 (21.5%), 4 (5.9%), 9 (21.5%), 21 (24.7%), 51 (100%), 54 (100%) and exports to the grid. This PFT is plotted in Fig. 8. At 5 pm this PV only feeds 45.6% of load 51.

Further conclusions may be inferred by means of the generator performance index. A generator engaged in multiple transactions is not necessarily performing well. Fig. 9 shows generators’ behavior in all DERs in the network from 10:30 am to 5:30 pm. To preserve comparability and hold the focus on losses, at those times when the network exports power to the grid, it has been considered a transaction with the substation.

TABLE VII
 TRANSACTIONS AT 12:30 PM AND AT 5 PM

		pv5	pv14	pv22	pv30	pv31	pv48	pv51	pv52	S/S
Load 1	12:30 pm		0.128	0.096	0.168	0.043	0.228	0.215	0.121	
	5 pm									1.000
Load 3	12:30 pm		0.128	0.096	0.168	0.043	0.228	0.215	0.121	
	5 pm									1.000
Load 4	12:30 pm	0.725	0.035	0.027	0.046	0.012	0.063	0.059	0.033	
	5 pm	1.000								
Load 5	12:30 pm	1.000								
	5 pm	1.000								
Load 9	12:30 pm		0.128	0.096	0.168	0.043	0.228	0.215	0.121	
	5 pm	0.190								0.810
Load 14	12:30 pm		1.000							
	5 pm		1.000							
Load 20	12:30 pm			1.000						
	5 pm			1.000						
Load 21	12:30 pm			0.111	0.193	0.049	0.262	0.247	0.139	
	5 pm	0.029	0.847							0.124
Load 22	12:30 pm			1.000						
	5 pm			1.000						
Load 25	12:30 pm				1.000					
	5 pm				0.921	0.079				
Load 29	12:30 pm					1.000				
	5 pm					1.000				
Load 30	12:30 pm				1.000					
	5 pm				1.000					
Load 31	12:30 pm					1.000				
	5 pm					1.000				
Load 34	12:30 pm				0.798	0.202				
	5 pm	0.005	0.159	0.041		0.771				0.023
Load 46	12:30 pm						1.000			
	5 pm						1.000			
Load 48	12:30 pm						1.000			
	5 pm						1.000			
Load 49	12:30 pm						1.000			
	5 pm						1.000			
Load 51	12:30 pm							1.000		
	5 pm	0.005	0.140				0.298	0.456	0.081	0.544
Load 52	12:30 pm								1.000	
	5 pm								1.000	
Load 54	12:30 pm						1.000			
	5 pm	0.009	0.257				0.547		0.149	0.038
Load 55	12:30 pm								1.000	
	5 pm								1.000	

S/S: secondary substation

DERs achieve the maximum performance index ($\xi_{pv} = 1$) when the prosumers’ load is bigger than its generation and all the power is used on-site. When the generation surpasses the consumption the power injected flows through the network feeding other loads and incurs in losses. The longer the path between peers trading an amount of power, the bigger the losses, pulling down the performance index of the generator. The worst generator performance index corresponds to pv51 at 12:30 pm ($\xi_{pv51} = 0.981$) when almost 2% of its generation is spent in losses through the network.

The transaction performance index becomes a valuable indicator, helpful to figure out if a transaction is worthwhile and determine the seller’s bid. Table VIII presents all transaction performance indices for pv51 at 12:30 pm. It is 100% for transactions close to the injection point. It drops to 93.66% in the transaction with Load3 at the head of the feeder. The power exported by pv51 to the grid has also been accounted. It has a transaction performance index of 97.83%, losses in the transformer and upstream were not considered though.

The dynamic DN-PFT energy transaction model contributes with understanding of the existing power transactions, determining their efficiency and supporting decision making. Thus,

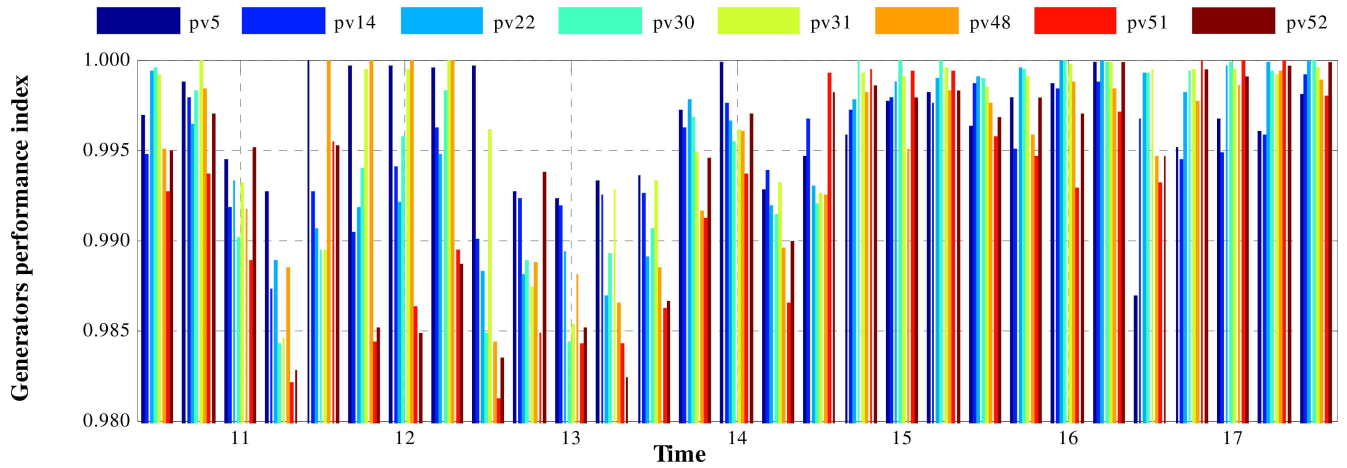


Fig. 9. Generators performance index in the modified IEEE European LV Test Feeder.

TABLE VIII
TRANSACTION PERFORMANCE INDICES AT 12:30 PM

	pv51- Load1	pv51- Load3	pv51- Load4	pv51- Load9	pv51- Load21	pv51- Load51	pv51- Load54	pv51- SS
Power supplied (kW)	0.045	0.013	0.174	0.151	0.066	0.060	0.054	2.151
Losses involved (W)	0.228	0.807	2.220	1.549	0.409	0	0	46.734
Transaction performance index (%)	99.50	93.66	98.72	98.97	99.39	100	100	97.83

loads close to PV generators could adjust their consumption profiles to the time periods of surplus generation while DERs with low demand in the surrounding could store the extra generation avoiding low performance transactions.

VI. CONCLUSION

In this article, a transaction-oriented dynamic power flow tracing model for DNs is proposed and implemented on open-source software packages. It aims to be of real application to support P2P energy trading, by quantifying the use of the distribution system and accounting for the losses incurred.

A new energy transaction model supported in PFT is defined. It identifies the power transactions existing in the network, quantifies the power reaching the loads from each source and apportions losses. The model unlocks flexible use of the surplus generation enabling prosumers to engage in P2P transactions with part of their production and sale the remaining power to the grid simultaneously. Two efficiency indices are defined to assess the performance of transactions and generators, they are helpful for prosumers to decide the mechanism for participation in energy trading.

The GIS platform displays power transactions enabling and encouraging transparent P2P engagements among prosumers, maximizing renewable energy usage. It helps DSOs to monitor the sources powering each line or load, coordinate the electricity market and efficiently manage interconnection requests. The tool includes feasibility validation of the transactions, preventing from violation of the network constraints or compromising DN operation.

A case study is conducted over the IEEE European LV Test Feeder. The tool developed provides a clear spatial and

temporal understanding of the power flows through the circuit. One moment a load can be fed by 8 generator (Load 4 at 12:30 pm) and later on just supplied from one generator (from pv5 at 5 pm). The tool determines the power transactions that are taking place, the losses share and the efficiency of DERs. It is found that pv51 at 12:30 pm shows the worst generator performance index, with almost 2% of its generation spent in losses through the network.

The potential benefits for DSOs and P2P energy trading of the dynamic PFT platform have been exposed on a feeder with limited number of distributed generators. Computational requirements when dealing with a whole DSO licensed area and the proliferation of various DERs will most likely need parallel processing which will be addressed in the coming platform release. Application layers over the GIS platform will be introduced such as optimization of DER planning and operation in DNs, to assess and support new market and regulations for reliable and efficient P2P energy trading and sharing. Future research will also include optimization of the prosumers' trading outcomes considering feasible P2P transactions, their performance and Fit/SEG to determine ask prices and base decision making.

REFERENCES

- [1] National Grid Electricity System Operator. (Jul. 2019). *Future Energy Scenarios*. Accessed: May 11, 2020. [Online]. Available: <http://fes.nationalgrid.com/media/1409/fes-2019.pdf>
- [2] W. Tushar, T. K. Saha, C. Yuen, D. Smith, and H. V. Poor, "Peer-to-peer trading in electricity networks: An overview," *IEEE Trans. Smart Grid*, vol. 11, no. 4, pp. 3185–3200, Jul. 2020.
- [3] W. Tushar *et al.*, "Grid influenced peer-to-peer energy trading," *IEEE Trans. Smart Grid*, vol. 11, no. 2, pp. 1407–1418, Mar. 2020.
- [4] J. Liang-Cheng, J. F. D. Rodrigues, and H. X. Lin, "Analysis of feed-in tariff policies for solar photovoltaic in China 2011–2016," *Appl. Energy*, vol. 203, pp. 496–505, Oct. 2017.
- [5] *Ofgem: Scheme Tariff Tables*. Accessed: Jul. 15, 2020. [Online]. Available: <https://www.ofgem.gov.uk/environmental-programmes/fit/fit-tariff-rates>
- [6] *British Gas: Our Tariffs*. Accessed: Jul. 15, 2020. [Online]. Available: <http://www.britishgas.co.uk>
- [7] Department for Business, Energy and Industrial Strategy. (Jun. 2019). *The Smart Export Guarantee Order 2019, No. 1005*. Accessed: Jul. 10, 2020. [Online]. Available: <https://www.legislation.gov.uk/uksi/2019/1005/made>
- [8] B. H. Rao, S. L. Arun, and M. P. Selvan, "Framework of locality electricity trading system for profitable peer-to-peer power transaction in

- locality electricity market,” *IET Smart Grid*, vol. 3, no. 3, pp. 318–330, Jun. 2020.
- [9] Y. Parag and B. K. Sovacool, “Electricity market design for the prosumer era,” *Nat. Energy*, vol. 1, no. 4, Apr. 2016, Art. no. 16032.
- [10] Y. Wang, W. Saad, Z. Han, H. V. Poor, and T. Başar, “A game-theoretic approach to energy trading in the smart grid,” *IEEE Trans. Smart Grid*, vol. 5, no. 3, pp. 1439–1450, May 2014.
- [11] N. Liu, X. Yu, C. Wang, C. Li, L. Ma, and J. Lei, “Energy-sharing model with price-based demand response for microgrids of peer-to-peer prosumers,” *IEEE Trans. Power Syst.*, vol. 32, no. 5, pp. 3569–3583, Sep. 2017.
- [12] B. Zhang, C. Jiang, J.-L. Yu, and Z. Han, “A contract game for direct energy trading in smart grid,” *IEEE Trans. Smart Grid*, vol. 9, no. 4, pp. 2873–2884, Jul. 2018.
- [13] W. Lee, L. Xiang, R. Schober, and V. W. S. Wong, “Direct electricity trading in smart grid: A coalitional game analysis,” *IEEE J. Sel. Areas Commun.*, vol. 32, no. 7, pp. 1398–1411, Jul. 2014.
- [14] J. Guerrero, A. C. Chapman, and G. Verbič, “Decentralized P2P energy trading under network constraints in a low-voltage network,” *IEEE Trans. Smart Grid*, vol. 10, no. 5, pp. 5163–5173, Sep. 2019.
- [15] C. Vartanian, R. Bauer, L. Casey, C. Loutan, D. Narang, and V. Patel, “Ensuring system reliability: Distributed energy resources and bulk power system considerations,” *IEEE Power Energy Mag.*, vol. 16, no. 6, pp. 52–63, Nov./Dec. 2018.
- [16] NERC. *Distributed_Energy_Resources_Report.pdf*. Accessed: Jul. 15, 2020. [Online]. Available: https://www.nerc.com/comm/Other/essntlrbltysrvckskfrcDL/Distributed_Energy_Resources_Report.pdf
- [17] A. Barbato *et al.*, “Lessons learnt from real-time monitoring of the low voltage distribution network,” *Sustain. Energy Grids Netw.*, vol. 15, pp. 76–85, Sep. 2018.
- [18] D. Apostolopoulou, S. Bahramirad, and A. Khodaei, “The interface of power: Moving toward distribution system operators,” *IEEE Power Energy Mag.*, vol. 14, no. 3, pp. 46–51, May/June 2016.
- [19] B. Meehan, *GIS for Enhanced Electric Utility Performance*. Boston, MA, USA: Artech House, 2013.
- [20] S. Lazarou, V. Vita, P. Karampelas, and L. Ekonomou, “A power system simulation platform for planning and evaluating distributed generation systems based on GIS,” *Energy Syst.*, vol. 4, no. 4, pp. 379–391, Dec. 2013.
- [21] L. Iyappan and P. K. Pandian, “Geoprocessing model for identifying potential wind farm locations,” *IET Renewable Power Gener.*, vol. 10, no. 9, pp. 1287–1297, Oct. 2016.
- [22] D. Palmer, E. Koumpli, I. Cole, R. Gottschalg, and T. Betts, “A GIS-based method for identification of wide area rooftop suitability for minimum size PV systems using LiDAR data and photogrammetry,” *Energies*, vol. 11, no. 12, p. 3506, Dec. 2018.
- [23] R. M. de Lima, R. Osis, A. R. de Queiroz, and A. H. M. Santos, “Least-cost path analysis and multi-criteria assessment for routing electricity transmission lines,” *IET Transm. Distrib. Gener.*, vol. 10, no. 16, pp. 4222–4230, Dec. 2016.
- [24] L. Yu *et al.*, “An efficient substation placement and sizing strategy based on GIS using semi-supervised learning,” *CSEE J. Power Energy Syst.*, vol. 4, no. 3, pp. 371–379, Sep. 2018.
- [25] J. Shu, L. Wu, Z. Li, M. Shahidehpour, L. Zhang, and B. Han, “A new method for spatial power network planning in complicated environments,” *IEEE Trans. Power Syst.*, vol. 27, no. 1, pp. 381–389, Feb. 2012.
- [26] J. B. Leite and J. R. S. Mantovani, “Detecting and locating non-technical losses in modern distribution networks,” *IEEE Trans. Smart Grid*, vol. 9, no. 2, pp. 1023–1032, Mar. 2018.
- [27] K. K. Radhakrishnan, J. Moirangthem, S. K. Panda, and G. Amaratunga, “GIS integrated automation of a near real-time power-flow service for electrical grids,” *IEEE Trans. Ind. Appl.*, vol. 54, no. 6, pp. 5661–5670, Nov./Dec. 2018.
- [28] G. Valverde, A. Arguello, R. González, and J. Quirós-Tortós, “Integration of open source tools for studying large-scale distribution networks,” *IET Gener. Transm. Distrib.*, vol. 11, no. 12, pp. 3106–3114, Aug. 2017.
- [29] R. C. Dugan and T. E. McDermott, “An open source platform for collaborating on smart grid research,” in *Proc. IEEE Power Energy Soc. Gen. Meeting*, 2011, pp. 1–7.
- [30] QGIS Development Team. *QGIS Geographic Information System. Open Source Geospatial Foundation Project*. Accessed: May 11, 2020. [Online]. Available: <http://qgis.osgeo.org>
- [31] QGIS. (Feb. 2016). *PyQGIS Developer Cookbook*. Accessed: May 11, 2020. [Online]. Available: <http://docs.qgis.org>
- [32] J. Bialek, “Tracing the flow of electricity,” *IEE Proc. Gener. Transm. Distrib.*, vol. 143, no. 4, pp. 313–320, Jul. 1996.
- [33] A. J. Conejo, J. M. Arroyo, N. Alguacil, and A. L. Guijarro, “Transmission loss allocation: A comparison of different practical algorithms,” *IEEE Trans. Power Syst.*, vol. 17, no. 3, pp. 571–576, Aug. 2002.
- [34] M. Usman, M. Coppo, F. Bignucolo, and R. Turri, “Losses management strategies in active distribution networks: A review,” *Electr. Power Syst. Res.*, vol. 163, pp. 116–132, Oct. 2018.
- [35] P. M. Costa and M. A. Matos, “Loss allocation in distribution networks with embedded generation,” *IEEE Trans. Power Syst.*, vol. 19, no. 1, pp. 384–389, Feb. 2004.
- [36] J. S. Savier and D. Das, “Impact of network reconfiguration on loss allocation of radial distribution systems,” *IEEE Trans. Power Del.*, vol. 22, no. 4, pp. 2473–2480, Oct. 2007.
- [37] J. Mutale, G. Strbac, S. Curcic, and N. Jenkins, “Allocation of losses in distribution systems with embedded generation,” *IEE Proc. Gener. Transm. Distrib.*, vol. 147, no. 1, pp. 7–14, Jan. 2000.
- [38] P. Kumar, N. Gupta, K. R. Niazi, and A. Swarnkar, “A circuit theory-based loss allocation method for active distribution systems,” *IEEE Trans. Smart Grid*, vol. 10, no. 1, pp. 1005–1012, Jan. 2019.
- [39] E. Carpaneto, G. Chicco, and J. S. Akilimali, “Branch current decomposition method for loss allocation in radial distribution systems with distributed generation,” *IEEE Trans. Power Syst.*, vol. 21, no. 3, pp. 1170–1179, Aug. 2006.
- [40] M. E. Baran and F. F. Wu, “Network reconfiguration in distribution systems for loss reduction and load balancing,” *IEEE Trans. Power Del.*, vol. 4, no. 2, pp. 1401–1407, Apr. 1989.
- [41] F. Milano and L. Vanfretti, “State of the art and future of OSS for power systems,” in *Proc. IEEE Power Energy Soc. Gen. Meeting*, 2009, pp. 1–7.
- [42] D. V. Nga, O. H. See, D. N. Quang, C. Y. Xuen, and L. L. Chee, “Visualization techniques in smart grid,” *Smart Grid Renewable Energy*, vol. 3, no. 3, pp. 175–185, Aug. 2012.
- [43] IEEE PES Distribution Systems Analysis Subcommittee Radial Test Feeders. *The IEEE European Low Voltage Test Feeder*. Accessed: Jul. 21, 2020. [Online]. Available: <https://site.ieee.org/pes-testfeeders/resources>

Eduardo Vega-Fuentes (Member, IEEE) received the M.Eng. and Ph.D. degrees in electrical engineering from the University of Las Palmas de Gran Canaria, Spain, in 1998 and 2015, respectively, where he was part-time Lecturer in systems engineering and automatics with the Department of Electronics Engineering and Automatics, from 2004 to 2018. He has been working as a Research Associate with the University of Glasgow, Scotland, U.K., since 2019. His research interests include energy conservation, optimal power systems operation, distribution automation, and smart grids.

Jin Yang (Senior Member, IEEE) received the B.Eng. and M.S. degrees in power systems from the North China Electric Power University, and the Ph.D. degree in electrical engineering from the University of Glasgow, Glasgow, U.K., in 2011, where he is currently a Senior Lecturer (Systems, Power and Energy) with the School of Engineering. His research focus is the power distribution network analysis, operation and control considering high penetration of distributed renewable energy resources, in research projects funded by UKRI, EPSRC, Royal Society, Horizon 2020 and industry. He is a holder of the EPSRC UKRI Innovation Fellowship (2018–2021), a Member of IET and Chartered Engineer (C.Eng.), and a Senior Fellow of Higher Education Academy (SF HEA).

Chengwei Lou received the B.S. and the M.E. degrees in electrical engineering and automation from China Agricultural University, Beijing, China. He is currently pursuing the Ph.D. degree in electrical engineering with the University of Glasgow. His current research interests include power distribution system modeling and optimization.

Nand K. Meena (Senior Member, IEEE) received the B.Tech.–M.Tech. (Dual) degrees in electrical engineering from IIT Kanpur, India, in 2011, and the Ph.D. degree in electrical engineering from the MNIT Jaipur, India, in 2018. He is currently a Marie Curie Fellow with the School of Engineering and Applied Science, Aston University, Birmingham, U.K. His research interests include optimization, planning and management of active distribution systems.